Structural analysis of in-plane loaded CLT beam with holes: FE-analyses and parameter studies

Jelec, Mario; Rajcic, Vlatka; Danielsson, Henrik; Serrano, Erik

Published in:
International Network on Timber Engineering Research - Proceedings Meeting 49

2016

Document Version:
Publisher's PDF, also known as Version of record

LUND UNIVERSITY

PO Box 117
221 00 Lund
+46 46-222 00 00

Structural analysis of in-plane loaded CLT beam with holes: FE-analyses and parameter studies

Mario Jelec, Department of Materials and Structures, University of Osijek, Croatia

Vlatka Rajcic, Department of Structures, University of Zagreb, Croatia

Henrik Danielsson, Division of Structural Mechanics, Lund University, Sweden

Erik Serrano, Division of Structural Mechanics, Lund University, Sweden

Keywords: cross laminated timber, CLT, in-plane loading, bending stress, shear stress, FE-analysis, holes, stress concentration, distribution of stress

1 Introduction

Thanks to its crosswise orientation, CLT is a very versatile material capable of carrying both in- and out-of-plane loads and can be used for wall or floor elements as well as for linear members. Despite its obvious benefits, the current status of CLT in European product and standard design still presents a major obstacle for developers, producers and designers, since properties and design for CLT have been regulated via national or international European Technical Approvals (ETAs). A product standard for CLT, EN 16351 (2015) has recently been published, but CLT is still not included in the European timber design code Eurocode 5, so further research, development and standardization work (including regulations for testing, design and execution), is needed (Brandner, 2016).

The aim of this paper is to investigate the performance of CLT beams with and without holes loaded in-plane under various loading conditions with special emphasis on shear loading and the in-plane shear behaviour considering the complex internal structure. CLT beams present a much better solution for beams with holes or notches as compared to glued laminated timber beams thanks to its lay-up where tensile forces perpendicular to the beam axis can be transferred by the transversal layers. In order to have in-depth understanding of the local mechanical behaviour in shear stress transfer between laminations, numerical analyses based on 3D-FE models are used.

FE-based approaches have been used previously for investigations of CLT behaviour (Blass and Görlacher 2002, Bejtka 2011, Flaig 2013) most of them being based on using beam elements or plane elements and not including the influence of e.g. the orthotropic material properties, beam build-up in the out-of-plane direction or stress distribution for various loading condition. Bejtka (2011) conducted comprehensive experimental and numerical analysis on cross and diagonal laminated timber beams, but since the work was focused more on determining bending strength and stiffness, complex shear stress states were not analysed completely.

2 Shear strength of CLT beams loaded in plane

In CLT beams exposed to in-plane loading normal and shear stresses occur. According to Schickhofer et al. (2010), Bogensperger et al. (2010), Flaig and Blass (2013) and Flaig (2013), verification of normal stresses in-plane only takes into account the bending resistance of the net cross section area, here meaning the layers in the direction of stresses. The contribution of the transverse layers (α=90°) is neglected because of the high MOE-ratio $E_0/E_{90}\approx30$. When it comes to verification of shear strength, calculation of shear stresses is however much more complicated. In general, according to Bogensperger et al. (2007, 2010), Flaig and Blass (2013) and Brandner et al. (2013) three different shear failure mechanisms have to be distinguished for CLT with and without adhesive bonding on the narrow face:

- Failure mode I (FM I) or gross shear failure of the CLT element by shear failures in all layers of CLT with narrow faces bonded layers
- Failure mode II (FM II) or net shear failure of the CLT element by shear failure in net cross sections of CLT
- Failure mode III (FM III) or torsion failure in the crossing areas between orthogonally bonded lamellae involving torsional and unidirectional shear stresses

2.1 Analytical approach

For evaluation of shear stresses in CLT wall element loaded in- plane, an efficient mechanical model for internal stress verification has been evaluated by Moosbrugger et al. (2006) and Bogensperger et al. (2007, 2010). Considering uniform shear loading on wall boundaries, an elementary representative volume sub element (RVSE) has been introduced, which presents the smallest unit cell at intersections between two orthogonal boards whose internal stress state describes the global stress state of the CLT element. In case of CLT beams, which are exposed to both bending and shear loading Flaig (2013) proposed a design procedure for verification of shear stresses, for each of the three failure modes. In case of FM I and FM II, shear stresses τ_{xy}, causing failure parallel and perpendicular to the grain, can be evaluated according to Bernoulli-Euler beam theory using the following expressions:

$$\tau_{xy,gross} = \frac{V_y \cdot S_{z,gross}}{I_{z,gross} \cdot t_{gross}} \qquad \text{(FM I)} \qquad (1)$$

$$\tau_{xy,net} = \frac{V_y \cdot S_{z,net}}{I_{z,net} \cdot t_{net}} \qquad \text{(FM II)} \qquad (2)$$

Maximum values of stresses can be calculated as peak values of the parabolic functions according to equation 3 and 4 (Fig. 1)

$$\tau_{xy,gross,max} = 1{,}50 \cdot \frac{V_y}{h \cdot t_{gross}} \qquad (3)$$

$$\tau_{xy,net,max} = 1{,}50 \cdot \frac{V_y}{h \cdot t_{net}} \qquad (4)$$

An example of shear stress distribution in the longitudinal and transversal layers of a CLT beam, with four lamellae in the longitudinal layers, is shown in Fig. 1. According to Flaig (2013) in case of even number of lamellae in longitudinal layers Eq. 3 overestimates the maximum shear stress in the gross cross section, where in case of odd number of lamellae in longitudinal layers, maximum net shear stresses are overestimated by Eq. 4.

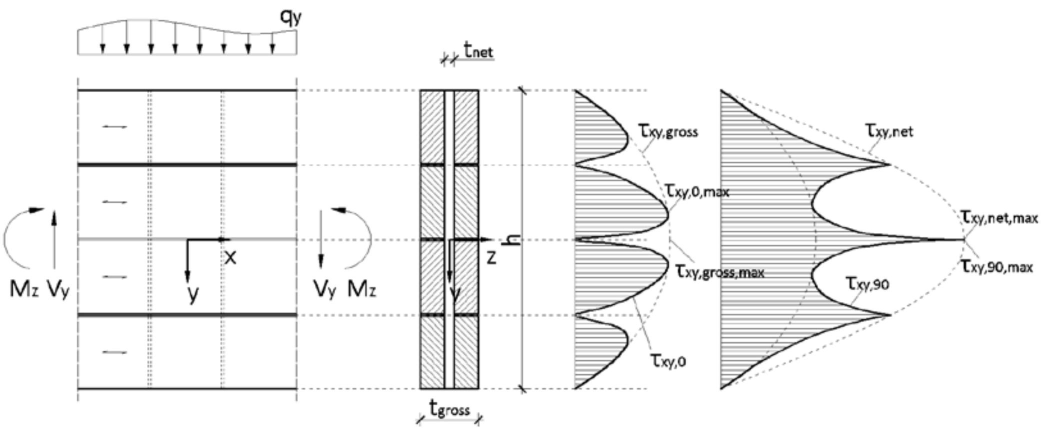

Figure 1. Distribution of shear stresses in the lamellae of CLT beam with four longitudinal lamellae: shear stresses $\tau_{xy,0}$ in longitudinal lamellae (left) and shear stress $\tau_{xy,90}$ in transversal lamellae (right)

In case of FM III, shear stresses originating from three different types of load transfer and acting in the crossing areas between the orthogonally bonded lamellae have to be considered (Flaig, 2013): shear stresses parallel to the beam axis (τ_{zx}), torsional shear stresses (τ_{tor}) and shear stresses perpendicular to the beam axis (τ_{zy}).

The shear stresses parallel to the beam axis, τ_{zx}, are caused by the change in the bending moment. The maximum values of the shear stress component τ_{zx} is found at the outermost lamellae of the beam and can be calculated according to:

$$\tau_{zx} = \frac{6V_y}{b^2 \cdot n_{CA}} \cdot \left(\frac{1}{m^2} - \frac{1}{m^3}\right) \qquad (5)$$

Torsional shear stresses, τ_{tor}, arise due to the eccentricity between the centre lines of adjacent lamellae. Flaig assumed equal torsional moments and hence equal torsional shear stresses for all crossing areas in the beam height direction, based on the condition that the lamellae in the transversal layers are assumed to remain straight in the deformed beam. The maximum torsional shear stress can then be calculated according to:

$$\tau_{tor} = \frac{3V_y}{b^2 \cdot n_{CA}} \cdot \left(\frac{1}{m} - \frac{1}{m^3}\right) \tag{6}$$

Shear stresses perpendicular to the beam axis, τ_{zy}, arise due to external concentrated forces, e.g. support reactions or external forces, or close to holes or notches. For a CLT beam without a hole or a notch and exposed to an external force q_y [N/m] applied to the end grain of the transversal layers, shear stresses can be evaluated according to Eq. 7 (Flaig, 2015).

$$\tau_{zy} = \frac{q_y}{m \cdot b \cdot n_{CA}} \tag{7}$$

In the design of CLT beams each of stress component must be verified with the corresponding shear strength related to relevant shear failure mode. Also, in the crossing areas interaction of shear stresses have to be considered (Flaig, 2013).

3 Shear strength of CLT beams with a hole

Flaig (2013) derived shear stress concentration factors for CLT beams with holes by performing numerical parameter analysis on girder FE-models (isotropic beam-spring models). In later work (Flaig, 2014) some additional idealisations were introduced, such as equal width *b* of all lamellae and constant ratio between the thickness of an individual longitudinal layer and the number of glue lines that the respective layer shares with adjacent transversal layers. The ratios $k_{h,1}$ and $k_{h,2}$, representing ratios of maximum shear stress at the hole to shear stress in an undisturbed beam of equal dimensions, were derived. The following equations for stress verification for CLT beams with holes were derived.

Bending stresses in the middle of the beam span and at the edge of the hole:

$$\sigma_{m,net} = \frac{M}{W_{net}} = \frac{24 \cdot F_{max}}{t_{net,0} \cdot h} \tag{8}$$

$$\sigma_{m,net,h} = \frac{15F_{max} \cdot h^2}{t_{net,0} \cdot (h^3 - h_h^3)} + \frac{3F_{max} \cdot h}{2 \cdot t_{net,0} \cdot h_r^2} \tag{9}$$

Tensile stresses perpendicular to beam axis:

$$F_{t,90} = F_V + F_M = F_{max}\left[\left(\frac{3h_h}{4h} - \frac{h_h^3}{4h^3}\right) + \left(\frac{0.008 \cdot x_h}{h_r}\right)\right] \tag{10}$$

$$\sigma_{t,90} = k_k \cdot \frac{F_{t,90}}{a_r \cdot t_{net,90}}; \text{with } a_r = \min\{b; 0.3(h + h_h)\} \tag{11}$$

Shear stresses (FM I, FM II and FM III):

$$\tau_{xy,gross,h} = 1{,}50 \cdot \frac{V_y}{(h - h_h) \cdot t_{gross}} \tag{12}$$

$$\tau_{xy,net,h} = k_{h2} \cdot \tau_{xy,net,max} = \left[0.103 \cdot \left(\frac{h_h \cdot l_h}{h^2} \cdot m^2\right) + 1.27\right] \cdot \tau_{xy,net,max} \tag{13}$$

$$\tau_{tor,h} = k_{h1} \cdot \tau_{tor} = \left[1.81 \cdot \left(\frac{l_h}{h} \cdot \frac{h_h}{h - h_h}\right) + 1.14\right] \cdot \tau_{tor} \tag{14}$$

$$\tau_{zx,h} = k_{h2} \cdot \tau_{zx} = \left[0.103 \cdot \left(\frac{h_h \cdot l_h}{h^2} \cdot m^2\right) + 1.27\right] \cdot \tau_{zx} \tag{15}$$

$$\tau_{zy,h} = \frac{F_{t,90}}{n_{CA} \cdot a_r \cdot h_r}; \text{with } h_r = \min\{h_{r,top}; h_{r,bottom}\} \tag{16}$$

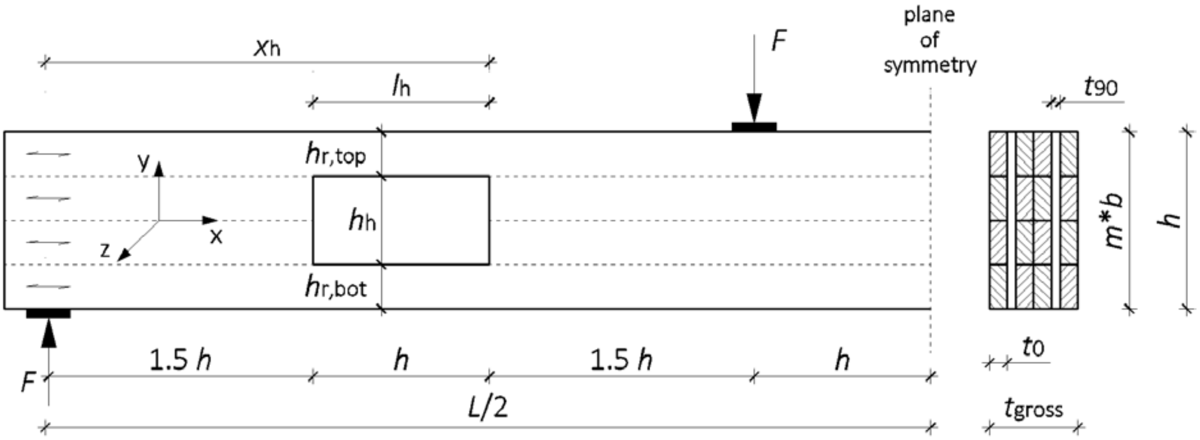

Figure 2. Geometry and layup of analyzed CLT beam

4 Numerical FE-analysis

CLT beams with and without holes were modelled. The CLT is modelled as a layered structure, each layer consisting of laminations (boards). The elements used are second order 3D elements (20-node) with full integration. The boards are assumed to be perfectly bonded only on their flat faces, while no edge bonding is assumed. Instead, a 0.1 mm gap between the boards within one layer is assumed. The perfect bond between the flat face areas of the boards was modelled by using contact elements in combination with perfect bonding and no sliding options of the software used (Ansys 17).The lamination material is assumed to be linear elastic and transverse isotropic. The material parameters are the same as used by Flaig (2014), strength class T14 according to EN 14080 see Table 1. The double symmetry of the test set-up is taken into account and thus only one quarter of each setup is modelled. Element mesh size was uniformly set to 5x5x5 mm^3 in the zones of relevance where stresses were evaluated, while in the more distant areas coarser mesh size was used.

Table 1. Material properties of longitudinal and transversal lamellae in N/mm^2

E_x	E_y	E_z	v_{xy}	v_{yz}	v_{xz}	G_{xy}	G_{yz}	G_{xz}
11000	370	370	0,35	0,35	0,35	690	69	690

5 Discussion and comparison of results

Results from the FE-analysis are presented below. The considered geometries and CLT lay-ups are the same as used for the experimental tests of CLT beams with holes reported by Flaig (2014). The stress values are calculated based on an applied load corresponding to the experimentally found mean failure loads. All stress components given below refer to the coordinate system shown in Fig. 2.

5.1 Bending stress analysis

Structural analysis on CLT beams was performed on six models whose dimensions, geometry and CLT lay-up are presented Table 2. In comparing the numerical results with the analytical, the mean value of bending stresses $\sigma_{m,net}$ over the net area at the mid span of the beam was calculated (Fig. 3) and compared with values obtained by Eq. 8.

Table 2. Dimension and layup of analysed CLT beams in [mm]

Model		h	h_h	h_r	t_{gross}	t_0	t_{90}	b	L	*layup*
without hole	H300	300	-	-	160	30	20	150	3150	l-c-l-l-c-l
	H600	600	-	-	150	30	15	150	6300	l-c-l-l-c-l
with hole	H300-0.4	300	120	90	160	30	20	150	3150	l-c-l-l-c-l
	H300-0.5	300	150	75	160	30	20	150	3150	l-c-l-l-c-l
	H600-0.4	600	240	180	150	30	15	150	6300	l-c-l-l-c-l
	H600-0.5	600	300	150	150	30	15	150	6300	l-c-l-l-c-l

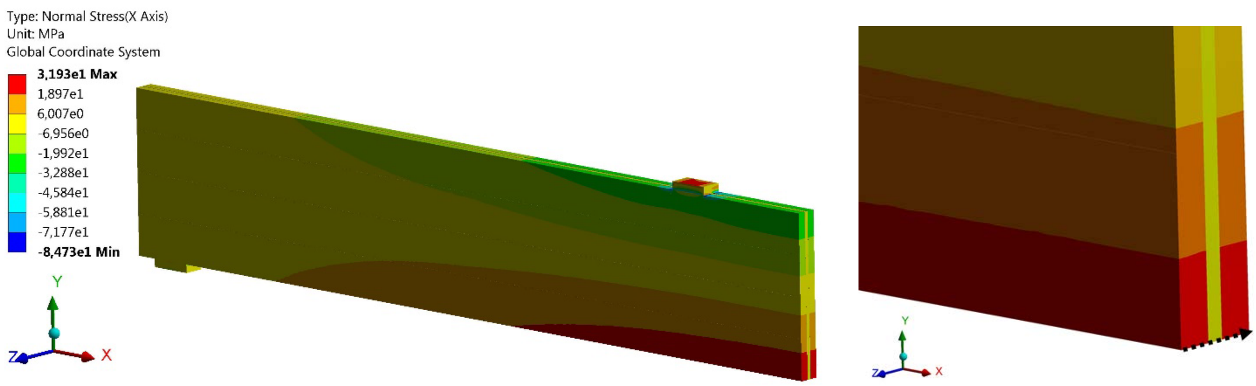

Figure 3. Normal stresses σ_x due to bending for model without hole H600 (left), and the stress path at the mid-span of beam for obtaining mean stress values (right)

In case of CLT beams with holes, additionally bending stresses at the edge of the hole further from the support, $\sigma_{m,net,h}$, were derived and compared with Eq. 9, which was proposed by Flaig (2014). Summarized results are presented in Table 3 and in general, a good agreement is obtained.

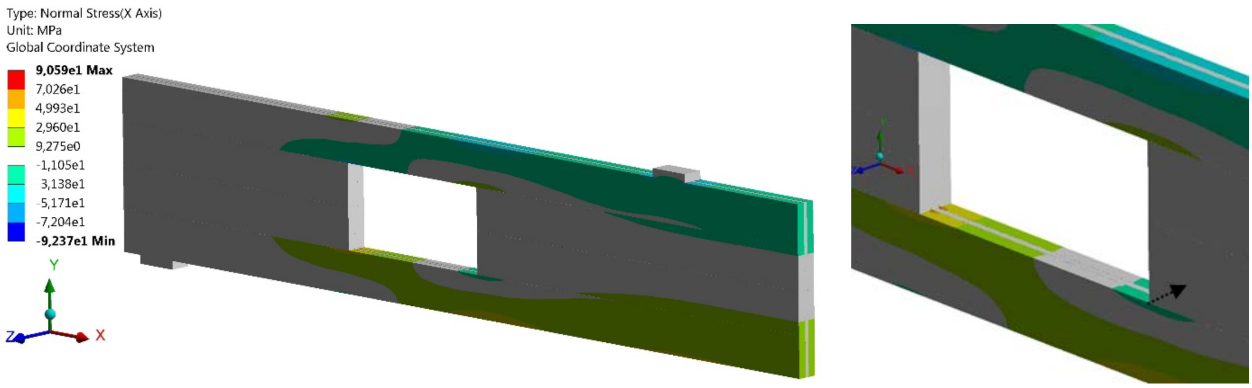

Figure 4. Normal stresses σ_x due to bending for model with hole H600-0.5 (left), and the stress path at the egde of the hole further from support for obtaining mean stress values (right)

Table 3. Summarized results of normal stresses σ_x due to bending

	Model	F_{max} [kN]	Numerical value [N/mm^2]		Analytical value [N/mm^2]	
			$\sigma_{x,net}$	$\sigma_{x,net,h}$	$\sigma_{m,net}$	$\sigma_{m,net,h}$
without hole	H300	59.70	41.59	-	39.80	-
	H600	85.46	29.89	-	28.48	-
with hole	H300-0.4	59.70	40.36	48.29	39.80	54.20
	H300-0.5	64.30	43.47	67.13	42.90	73.50
	H600-0.4	109.76	37.29	47.76	36.62	49.88
	H600-0.5	85.46	28.94	47.05	28.48	48.84

5.2 Tensile stress perpendicular to the beam axis

For CLT beams with holes, tensile stress acting perpendicular to the beam axis at the vertical edges of the holes were calculated according Eq. 10, which is given in the German National Annex (NA) to Eurocode 5 for glulam beams with holes. Since numerical results were mesh size sensitive and high stress concentrations were obtained (Fig. 5), the mean tensile stress in the transversal lamellae at the edges of the holes was calculated according to Eq. 17 and compared with analytical values (Fig. 5).

$$\sigma_{y,90,mean} = \frac{\int \sigma_{y,90}}{A} = \frac{F_{t,90}}{a_r \cdot t_{90}} \qquad (17)$$

The tensile stress in the transversal lamellae was calculated using an effective width, a_r, which is chosen as the smaller value of the actual width of the lamellae and the maximum value given in the German NA to EC5 for glulam beams with reinforced holes. The highly non-uniform distribution of tensile stresses is accounted for in the German NA with a factor k_k = 2.0 (Eq. 11).The mean stress from the FE-model was thus compared with the mean analytical value by neglecting the factor k_k. The results are presented in Table 4, showing in general a good agreement with the analytical results.

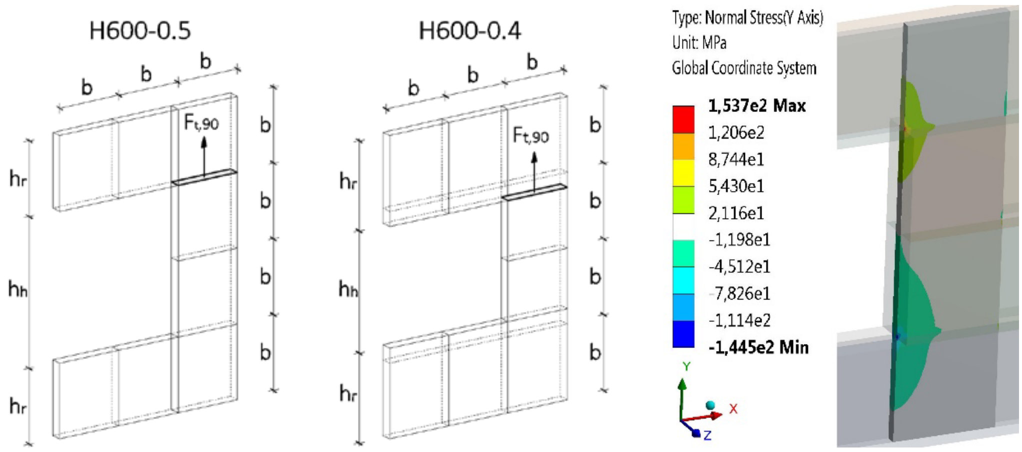

Figure 5. Cross-section area for determining total tensile force perpendicular to beam axis, $F_{t,90}$, (left) and obtained stress concetration at corner of hole for model H600-0.5 (right)

Table 4. Summarized results of tensile stresses perpendicular to beam axis $\sigma_{t,90}$

Model	F_{max} [kN]	Numerical value		Analytical value		
		$F_{t,90}$ [kN]	$\sigma_{t,90,mean}$ [N/mm^2]	$F_{t,90}$ [kN]	$\sigma_{t,90,mean}$ [N/mm^2]	$\sigma_{t,90}$ [N/mm^2]
H300-0.4	59.70	7.99	3.17	10.46	4.15	8.30
H300-0.5	64.30	13.07	4.84	13.11	4.85	9.71
H600-0.4	109.76	19.86	8.82	19.28	8.57	17.14
H600-0.5	85.46	26.40	11.73	18.10	8.04	16.10

5.3 Shear stress analysis

In shear stress analysis, verification of each stress component was done, including shear stresses in gross and net sections as well as over crossing areas of laminations. For models without holes, shear stresses τ_{xy} and τ_{zx} in transversal lamellae located between the load point and support are presented in Fig. 6, while for models with holes shear stresses τ_{xy}, τ_{zx} and τ_{zy} in the first transversal lamellae near the hole are presented in Fig. 7. The distribution of shear stresses τ_{xy} across the beam height is also presented over four different stress paths in Fig. 8, with the following meaning a) at the surface of longitudinal lamellae, b) at the centre of longitudinal lamellae, c) at the surface of transversal lamellae (over crossing areas) and d) at the centre of transversal lamella. Stress paths are marked as black arrows in Fig. 6 and Fig. 7.

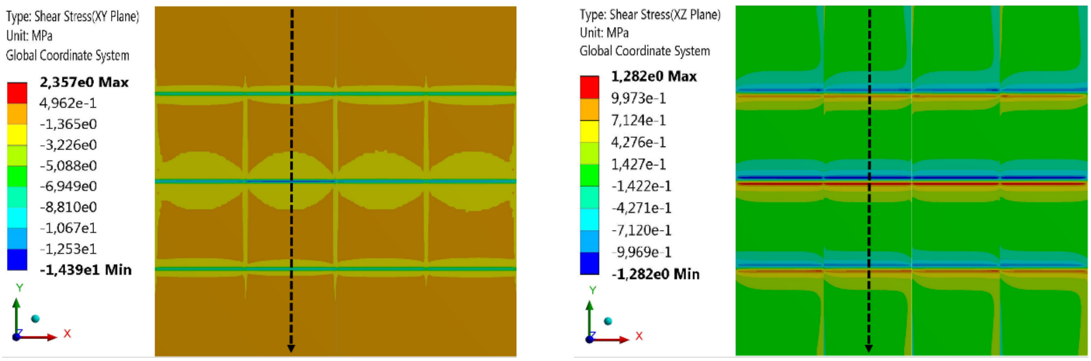

Figure 6. Results of shear stresses τ_{xy} (left) and shear stresses τ_{zx} (right) in model H600

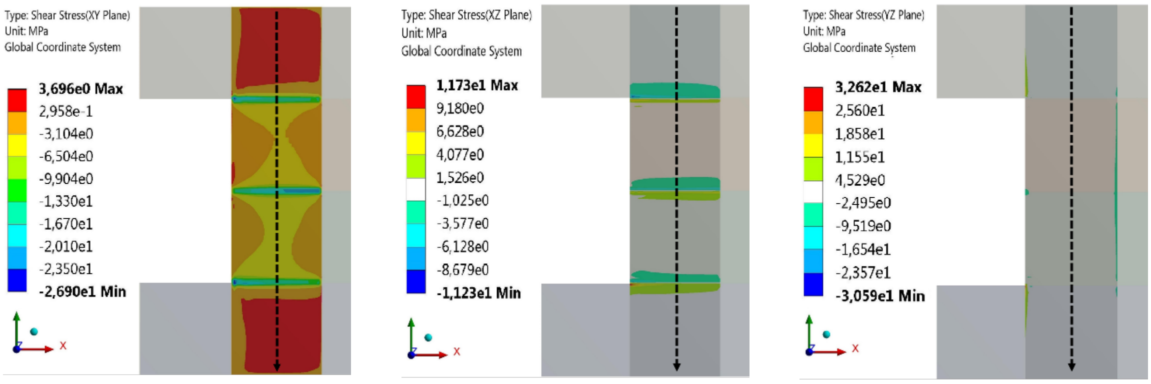

Figure 7. Results of shear stresses τ_{xy}, τ_{zx} and τ_{zy} in model H600-0.5 (from left to right)

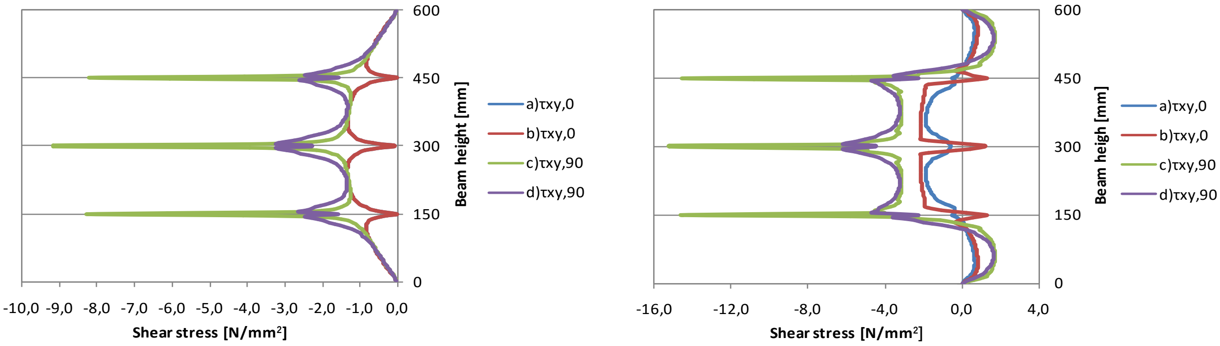

Figure 8. Distribution of shear stresses τ_{xy} across the beam height over four different stress paths (H600 - left, H600 - 0.5 - right)

From the presented distributions some differences may be noticed comparing models with and without holes. In models with holes the distribution of shear of stress τ_{xy} is slightly disturbed due to the small distance to the hole and higher peak values may be noticed. When it comes to shear stress τ_{zx}, from Fig. 9 (left) it may be noticed that for models without holes the maximum value occurs at the center of the beam, which is not in accordance with Flaig`s assumption explained earlier. In case of models with holes, maximum values occur at sections that are coincident with the edges of the hole (Fig. 9 (right)), with concentration of stresses at the corner of the hole. In general, from all the presented graphs, a non-uniform stress distribution may be noticed. From this reason, in verification of each failure mode (FM I, FM II and FM III) mean stresses over appropriate areas or paths were derived and compared with analytical values.

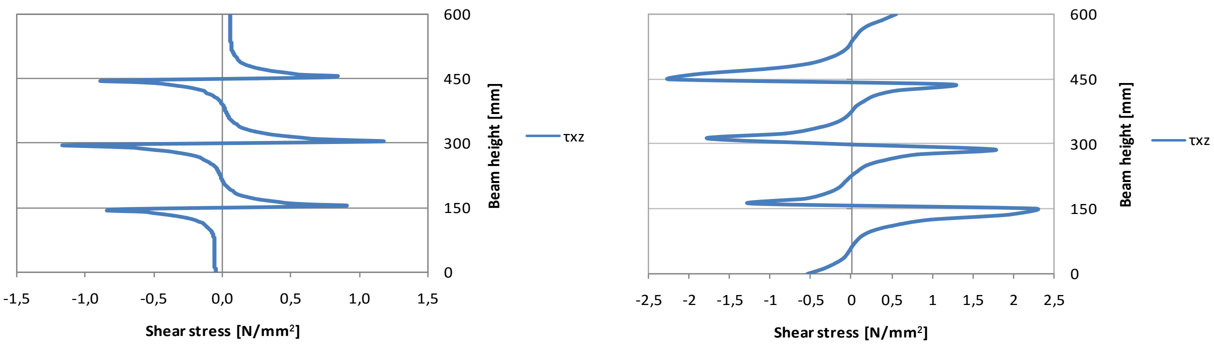

Figure 9. Distribution of shear stresses τ_{zx} across the beam height (H600 - left, H600-0.5 - right)

5.3.1 *Verification of FM I*

In case of CLT beams without holes, the maximum value of shear stress $\tau_{xy,0}$ along a stress path across the centre of the longitudinal lamellae (curve b) of Fig. 8 (left)) is compared with the analytical values (Eq. 3). For CLT beams with holes, the distribution of shear stresses $\tau_{xy,0}$ over beam height in the section that passes through the hole is presented in Fig. 10. The mean value of gross shear stress over the beam thickness was calculated (Fig. 10) and compared with the analytical equation (Eq. 12). Summarized results are presented in Table 5 and in general, a good agreement is obtained. In the case of model H300 the difference is 11.03%, while the expected error is 25% (Flaig, 2013). For model H600 the difference is smaller, 5.75%, and close to the predicted error 6.3% (Flaig, 2013). For models with holes, differences are even smaller and are for each of the analysed model below 5%.

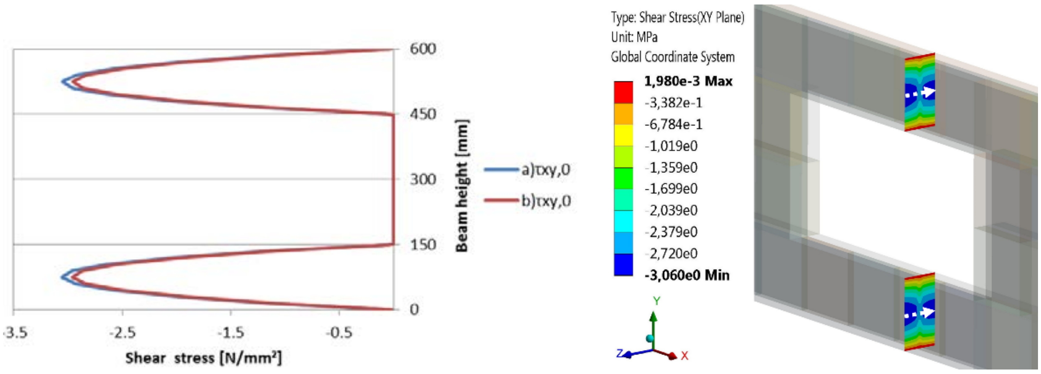

Figure 10. Distribution of shear stress τ_{xy} over beam height (left) and stress path marked as arrow for determining mean values in beam thickness direction (right)

Table 5. Summarized results of shear stresses τ_{xy} for verification of FM I

	Model	F_{max} [kN]	Numerical value [N/mm^2]		Analytical value [N/mm^2]
			$\tau_{xy,0,max}$	$\tau_{xy,0,mean}$	$\tau_{xy,gross}$
without hole	H300	59.70	1.66	-	1.86
	H600	85.46	1.34	-	1.42
with hole	H300-0.4	59.70	3.48	3.01	3.11
	H300-0.5	64.30	4.54	4.04	4.02
	H600-0.4	109.76	3.10	3.05	3.05
	H600-0.5	85.46	2.96	2.86	2.85

5.3.2 *Verification of FM II*

In relation to FM II, evaluation of the maximum value of the net shear stress $\tau_{xy,net}$ according to the FE-analyses is problematic since the stress distribution is highly non-uniform and much affected by e.g. the discontinuities introduced by the gaps between the lamellae. Thus, mean values of net shear stresses $\tau_{xy,net}$ across the critical cross sections of the transversal lamellae were obtained by integration of stresses (see Fig. 11). These correspond then to the total (resultant) shear force F_{xy} divided by cross section area of the transversal lamellae according to Eq. 18. Summarized results are presented in Table 6. From presented results, general good agreement is obtained except in the case of model H600-0.4 and H600-0.5 where larger difference may be noticed. Possible reason of that could be influence of mesh size, since using a finer mesh, the numerical values get closer to analytical ones.

$$\tau_{xy,net,mean} = \frac{\int \tau_{xy}}{A} = \frac{F_{xy}}{b \cdot t_{90}} \tag{18}$$

Table 6. Summarized results of net shear stresses τ_{xy} for verification of FM II

	Model	F_{max} [kN]	Numerical value [N/mm²] $\tau_{xy,net,mean}$	Analytical value [N/mm²] $\tau_{xy,net}$
without hole	H300	59.70	7.46	7.36
	H600	85.46	6.76	7.12
with hole	H300-0.4	59.70	11.22	10.71
	H300-0.5	64.30	12.68	11.86
	H600-0.4	109.70	14.96	17.54
	H600-0.5	85.46	12.34	14.91

5.3.3 *Verification of FM III*

In case of FM III, according to Flaig (2013) interaction between shear stresses in beam direction τ_{zx} and torsion shear stresses τ_{tor} should be verified over crossing areas. From the FE-results, the relevant shear stress components can of course be directly evaluated in relation to the corresponding strength values, without decomposing them into transverse, longitudinal and torsional shear. For comparison with analytical expressions, however, mean stress values were calculated by integration of stresses over each crossing area (Fig 11). In that sense, the total (resultant) shear forces F_x and F_y were obtained and divided with crossing areas (Eq. 19 and 20). From the FE-software the torsional moment M_{tor} could be obtained and torsion stresses were calculated according to Eq. 21 (Blass, 2002). Results are given in Table 7.

$$\tau_{zx,\mathrm{cross},mean} = \frac{\int \tau_{zx}}{A_{cross}} = \frac{F_x}{b \cdot b} \tag{19}$$

$$\tau_{zy,\mathrm{cross},mean} = \frac{\int \tau_{zy}}{A_{cross}} = \frac{F_y}{b \cdot b} \tag{20}$$

$$\tau_{tor} = \frac{M_{tor}}{I_p} \cdot \frac{b}{2} \tag{21}$$

From Table 7 it may be noticed that torsional stresses are not equal over each crossing area and for model H600 they are higher close to the neutral axis. In case of shear stress τ_{zy} in models without holes, the obtained numerical values are quite small, in accordance with theoretical background. For models with holes for torsion shear stresses τ_{tor} a larger difference between numerical and analytical results may be noticed. A possible reason for this is the position and size of the hole in relation to crossing areas of first neighbouring vertical lamellae. Other reasons could be the influence gap size between laminations and width of first vertical lamellae near the hole since these parameters were not known completely. Since the analytical approach is based on a girder model, and involves some idealizations, the real arrangement of the longitudinal and transversal laminations is not taken into account. The presented numerical analysis was done on a limited number of models, so a more comprehensive parameter analysis should be carried out to validate the FE-model.

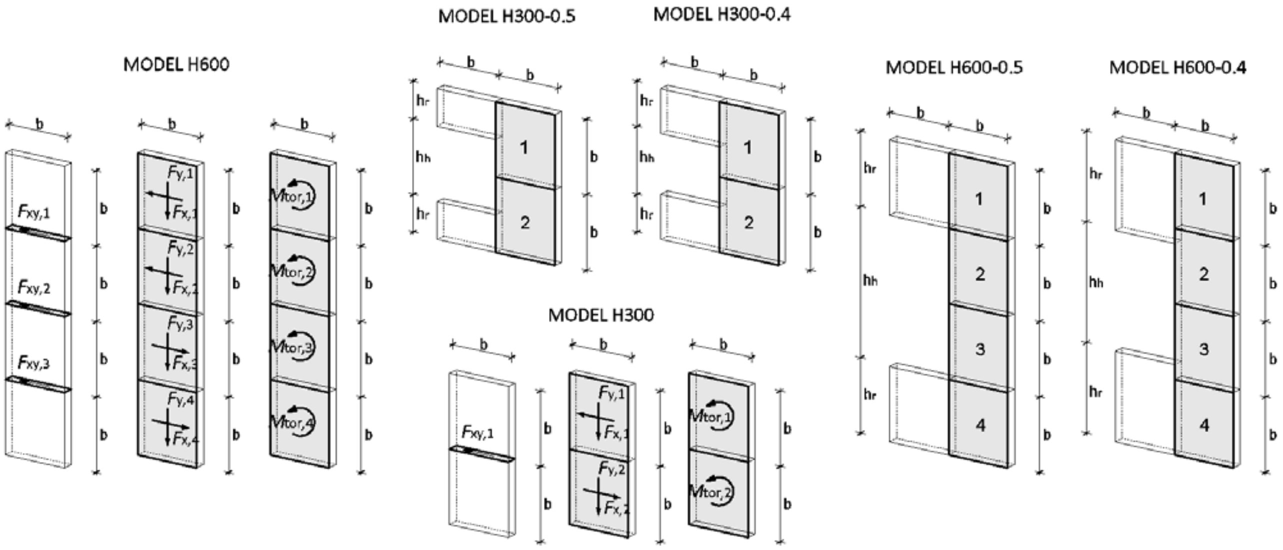

Figure 11. Cross-sectional areas for obtaining resultant forces in verification of FM II and FM III

Table 7. Summarized results of shear stresses over crossing areas for verification of FM III

	Model	F_{max}	Cross. area	Numerical results [N/mm^2]			Analytical results [N/mm^2]		
				$\tau_{zx,mean}$	τ_{tor}	$\tau_{zy,mean}$	τ_{zx}	τ_{tor}	τ_{zy}
without holes	H300	59.70	1	0.48	0.79	0.06	0.49	0.75	-
			2	0.48	0.79	0.05			
	H600	85.46	1	0.26	0.32	0.04	0.26	0.67	-
			2	0.07	0.69	0.01			
			3	0.07	0.68	0.01			
			4	0.26	0.32	0.05			
with holes	H300-0.4	59.70	1	0.73	1.11	0.25	0.71	1.75	0.29
			2	0.72	1.11	0.29			
	H300-0.5	64.30	1	0.81	1.24	0.43	0.79	2.37	0.51
			2	0.81	1.24	0.51			
	H600-0.4	109.70	1	0.28	0.90	0.38	0.66	2.01	0.35
			2	0.46	0.90	0.35			
			3	0.45	0.91	0.36			
			4	0.29	0.91	0.41			
	H600-0.5	85.46	1	0.49	1.43	0.48	0.55	1.96	0.40
			2	0.13	1.11	0.50			
			3	0.12	1.11	0.50			
			4	0.50	1.43	0.49			

6 Conclusions and further work

In general, for CLT beams without holes, the obtained results are in good agreement with simplified analytical values proposed by Flaig (2013). The main difference relates to the distribution of shear stresses τ_{zx} over the crossing areas per height of CLT beam, where the maximum value is found to be in middle of beam height in contradiction with the assumption of Flaig. For CLT beams with holes, the obtained results are in good agreement with analytical values except the torsion shear stresses over the crossing area of transversal lamellae near the hole. The analytical values were smaller in all cases since they were obtained by Eq.19, which does not consider stress concentrations. The real arrangement of the longitudinal and transversal lamellae in relation to the hole position is a second reason for the difference observed. The analytically derived equations are namely based on idealised girder models which cannot model an arbitrary hole position. In case of tensile stress perpendicular to beam axis, the tensile force was calculated according to German NA to EC5 for glulam beams with holes. Since the failure mechanism for glulam and CLT beams with holes is different, the proposed equations should be validated on a larger number of CLT models. For the presented limited number of models, the agreement between mean values is acceptable, even if high stress concentrations at the corner of the holes were obtained. The presented analyses are a first attempt to contribute to the on-going review process of Eurocode 5 as regards CLT beams with holes. Currently there are no regulations on how to design such beams, so further experimental and numerical investigations are planned.

7 Symbols

t_{gross}	total thickness of CLT beam	h_h	hole height
t_{90}	thickness of vertical lamellae	l_h	length of hole
t_0	thickness of longitudinal lamellae	b	width of lamellae
t_{net}	smaller of the sum of the thickness of longitudinal and transversal layers	x_h	distance of further edge of hole from support
$t_{net,0}$	sum of the thickness of longitudinal lamellae	$h_{r,t/b}$	residual height above or below the hole (*t* - top, *b* - bottom)
$t_{net,90}$	sum of the thickness of transversal lamellae	I_z	second moment of inertia about z-axis
		S_z	static moment about z-axis
n_{CA}	number of crossing areas within beam thickness	m	number of longitudinal lamellae within the beam height

8 References

Bejtka, I (2011): Cross (CLT) and diagonal (DLT) laminated timber as innovative material for beam elements. Karlsruher Berichte zum Ingenieurholzbau, Bd. 17, KIT Scientific Publishing

Blass, H-J, Görlacher, R (2002): Zum Trag- und Verformungverhalten von Brettsperrholz-Elementen bei Beanspruchung in Plattenebene. Bauen mit Holz, 12:30-34

Bogensperger, T, Moosbrugger, T, Silly, G (2010): Verification of CLT-plates under loads in plane. In: Proc. 11th World Conference on Timber Engineering, Riva del Garda, Italy.

Bogensperger, T, Moosbrugger, T, Schickhofer, G (2007): New Test Configuration for CLT-Wall Elements under Shear Load. In: Proc. CIB-W18 Meeting 40, Bled, Slovenia, Paper 40-12-3

Brandner, R, Bogensperger, T, Schickhofer, G (2013): In plane Shear Strength of Cross Laminated Timber (CLT): Test Configuration, Quantification and influencing Parameters. In: Proc. CIB-W18 Meeting 46, Vancouver, Canada, Paper 46-12-2

Brandner, R, Flatscher, G, Ringhofer, A, Schickhofer, G, Thiel, A (2016): Cross laminated timber (CLT): overview and development. European Journal of Wood and Wood Products, 74:331-351

DIN EN 1995-1-1/NA (2013) National Annex – Nationally determined parameters – Eurocode 5: Design of timber structures – Part 1-1: General – Common rules and rules for buildings. (DIN)

EN 16351 (2015) Timber structures – Cross laminated timber – requirements (CEN)

EN 14080 (2013) Timber Structures – Glued laminated timber and glued solid timber – Requirements (CEN)

ETA-12/0281, “NORITEC X-LAM” (2012): Cross Laminated Timber (CLT) – Solid wood slab elements to be used as structural elements in buildings”, NORITEC Holzindustrie GmbH, Österreichisches Institut für Bautechnik (OIB).

Eurocode 5 (2004): Design of timber structures - Part 1-1: General and rules for buildings. European Committee for Standardization (EN 1995-1-1)

Flaig, M, Blass, H-J (2013): Shear strength and Shear stiffness of CLT beams loaded in plane. In: Proc. CIB-W18 Meeting 46, Vancouver, Canada, Paper 46-12-3

Flaig, M (2013): Biegeträger aus Brettsperrholz bei Beanspruchung in Plattenbene. Dissertation, Karlsruher Berichte zum Ingenieurholzbau, Bd. 26, KIT Scientific Publishing

Flaig, M (2014): Design of CLT Beams with Rectangular Holes or Notches, In: Proc. 1st INTER Meeting, Bath, United Kingdom, Paper 47-12-4

Flaig, M (2015): In Plattenebene beanspruchte Biegeträger aus Brettsperrholz. Bautechnik, 92:741-749

Moosbrugger, T, Guggenberger, W, Bogensperger, T (2006): Cross Laminated Timber Wall Segments under homogeneous Shear – with and without Openings. In: Proc. 9th World Conference on Timer Engineering, Portland, Oregon, USA

Schickhofer, G, Bogensperger, T, Moosburger, T (2010): BSPhandbuch (CLThandbook: solid timber construction technique with cross laminated timber – verification base on new European standardization concept). Verlag der Technischen Universität Graz (in German)